Environmental Science
Processes & Impacts

Oil & Gas Produced Water Retention Ponds as Potential Passive Treatment for Radium Removal and Beneficial Reuse

Journal:	*Environmental Science: Processes & Impacts*
Manuscript ID	EM-ART-09-2020-000413.R2
Article Type:	Paper

Oil & Gas Produced Water Retention Ponds as Potential Passive Treatment for Radium Removal and Beneficial Reuse

Bonnie McDevitt[1], Molly C. McLaughlin[2,3], Jens Blotevogel[3], Thomas Borch[3,4,5], Nathaniel R. Warner[1]*

[1] Department of Civil and Environmental Engineering, The Pennsylvania State University, 212 Sackett Building, University Park, PA 16801, USA
[2] Abt Associates Inc., 2755 Canyon Blvd., Boulder, CO, 80301
[3] Department of Civil and Environmental Engineering, Colorado State University, 1170 Campus Delivery, Fort Collins, CO, 80523-1170, USA
[4] Department of Soil and Crop Sciences, Colorado State University, 1170 Campus Delivery, Fort Collins, Colorado 80523, USA
[5] Department of Chemistry, Colorado State University, 1872 Campus Delivery, Fort Collins, Colorado, 80523, USA

*corresponding author, nrw6@psu.edu

Abstract

Oil and gas (O&G) extraction generates large volumes of produced water (PW) in regions that are often water-stressed. In Wyoming, generators are permitted under the National Pollutant Discharge Elimination System (NPDES) program to discharge O&G PW for beneficial use. In one Wyoming study region, downstream of the NPDES facilities exist naturally occurring wetlands referred to herein as produced water retention ponds (PWRPs). Previously, it was found that dissolved radium (Ra) and organic contaminants are removed within 30 km of the discharges and higher-resolution sampling was required to understand contaminant attenuation mechanisms. In this study, we sampled three NPDES discharge facilities, five PWRPs, and a reference background wetland not impacted by O&G PW disposal. Water samples, grab sediments, sediment cores and vegetation were collected. No inorganic PW constituents were abated through

the PWRP series but Ra was shown to accumulate within PWRP grab sediments, upwards of 2,721 Bq/kg, compared to downstream sites. Ra mineral association with depth in the sediment profile is likely controlled by the S cycle under varying microbial communities and redox conditions. Under anoxic conditions, common in wetlands, Ra was available as an exchangeable ion, similar to Ca, Ba and Sr, and S was mostly water-soluble. ^{226}Ra concentration ratios in vegetation samples, normalizing vegetation Ra to sediment Ra, indicated that ratios were highest in sediments containing less exchangeable ^{226}Ra. Sequential leaching data paired with redox potentials suggest that oxic conditions are necessary to contain Ra in recalcitrant sediment minerals and prevent mobility and bioavailability.

Environmental Significance Statement

Beneficial reuse of oil and gas produced water in the U.S. is increasingly being considered outside the oil and gas industry. Though study site TDS concentrations of produced water discharges were low, downstream SO_4, Cl and Na concentrations exceeded livestock drinking water guidelines. Similarly, though discharges contained low dissolved total radium concentrations, radium significantly accumulated in sediments downstream. Wetlands can act as a contaminant sink for radium if kept oxic, potentially providing a low-cost and sustainable produced water polishing treatment. Wetland vegetation significantly accumulated radium-226 upwards of 880 Bq/kg. Because cattails remain an important food source for some mammals, the observed radium accumulation in wetland vegetation could provide significant radium exposure to local wildlife if proper exclusion methods are not employed.

Introduction

Oil and gas (O&G) produced water (PW) is the largest byproduct the industry generates with an estimated 3 billion m^3 PW/year [1] – domineering volumes of oil and gas extracted, frequently by magnitudes. The economic decision for continuing O&G well production is often based on the total dissolved solids (TDS) composition and regionally available options for PW disposal: industry recycling, deep well injection, beneficial use, or surface water discharge. Deep well injection is the most common disposal option (>90%) for U.S. unconventional PW, although the practice is increasingly criticized for creating large deficits in local water cycles[2,3] and induced seismicity[4]. Treatment of PW can range from U.S. \$1-15/m^3 [5] and is necessary when considering industry recycling, beneficial use or surface water discharge. Currently, only Wyoming and Pennsylvania allow for the disposal of treated PW to surface water streams, although an increasing number of states are seeking legislature approval of the practice.

As encompassed in the term "water-energy-food nexus", O&G extraction activities often occur in regions that experience extreme water stress, such as Western U.S. shale basins (i.e. Bakken, Niobrara, Permian, and Eagle Ford) [2]. In such areas, PW can contribute a significant volume of water to local agricultural economies. Preventing permanent loss of water from local water cycles in arid and semi-arid regions, where water is arguably a more valuable commodity than oil or gas and at times a legal challenge, remains an important turning point for the future of the O&G industry. Government foresight by the U.S. Geological Survey, U.S. Department of Energy, and U.S. Environmental Protection Agency to recycle and reuse PW is evidenced in the

recent increase in related research requests for proposals and plans [6–9]. Western U.S. states beneficially reuse PW for agriculture and wildlife propagation under the NPDES exemption 40 CFR § 435 Subpart E. Irrigation studies have reported diverging results on the use of PW on soil and plant health. Kondash et al. (2020) established no significant differences in soil chemistry other than elevated boron and sodium between the use of blended O&G PW or regional groundwater as irrigation in California's Central Valley [10]. However, another recent study suggested that O&G PW blended with freshwater led to reduced soil health, reduced crop health, and a significant shift in the soil microbial community between irrigation treatments [11]. Furthermore, several produced water studies have reported ecotoxicity to *Daphnia magna*, rainbow trout, and fatmucket (*Lampsilis siloquoidea*) freshwater mussels including oxidative stress, physical immobility, and mortality [12–15].

Wyoming has approximately 500 NPDES facilities for the disposal of PW permitted through the beneficial use exemption, though during the height of coalbed methane (CBM) production in Wyoming, the number of permitted facilities was greater than 1000. A remote study region in Wyoming described previously by McDevitt et al. (2019, 2020b) and McLaughlin et al. (2020a, 2020b) includes PW discharges to ephemeral draws and downstream vegetated produced water retention ponds (PWRPs). Some of the PWRPs were created in partnership with the U.S. Fish and Wildlife Service to provide habitat for migratory birds and other wildlife and other PWRPs that have naturally formed from years of periodically saturated soils [16–19]. McDevitt et al. (2020b) characterized seven NPDES discharges of PW, respective discharge streams, and two regional perennial rivers utilizing stable isotopes $\delta^{18}O$, $\delta^{2}H$, $\delta^{34}S_{SO4}$, $\delta^{7}Li$ and radiogenic

$^{87}Sr/^{86}Sr$. Isotopic signatures supported evaporation of PW along all discharge streams and oxidation of PW-derived sulfide gas within the discharge stream leading to increasing SO_4 concentrations. McLaughlin et al. (2020a, 2020b) described one NPDES discharge and its PW ephemeral stream in detail regarding degradation of organic contaminants with increasing distance downstream associated with decreasing mutation rates in yeast cells[18,19]. The current study was conducted based on guidance from results of previous studies that indicated higher distance resolution within the PW streams near NPDES discharges was necessary to understand contaminant sequestration. Additionally, Ra removal mechanisms related to the existence of PWRPs within the PW stream were acknowledged data gaps. Other regional studies reported issues associated with inefficient oil-water separation systems in Wyoming that discharged remnant oil into downstream wetlands, which led to mortality of wildlife, namely birds [20]. It was also noted that Ra accumulated in some Wyoming PW wetland sediments and through the aquatic food chain with upwards of 1,110 Bq/kg in vegetation and 37 Bq/kg in bird bones [21].

McDevitt et al. (2019) reported that even low Ra activities in fluids that were discharged to the ephemeral draws in this study region of Wyoming led to significantly elevated sediment Ra activities compared to background sediments, upwards of 50 times higher [16]. Moreover, McDevitt et al. (2019) found that, near a discharge, approximately 75% of the sediment Ra was associated with sediments comprising >97% calcium carbonate minerals. However, only 5% of the annually discharged Ra was attenuated within 100 m of the discharge, indicating mobility and transport of the remaining 95% of the annual Ra load, either as an aqueous species or more likely fine particle-associated.

The PW stream Ra sediment activities were, however, attenuated to background levels within 2 km of one NPDES discharge and within 30 km at another NPDES discharge. Geochemical modeling from McDevitt et al. (2019) indicated the dominance of Ra attenuation with distance by co-precipitation with carbonate minerals and to a lesser extent with sulfate minerals in the form of barite solid solutions[16].

From McDevitt et al. (2019) it was recommended that the study site NPDES treatment facilities include construction of polishing wetlands or filtration ponds just below the discharge into the PW stream, which would allow for establishment of chemical and equilibrium conditions (i.e. temperature cooling, increased oxygen concentrations, oxidation of sulfide gas to sulfate in-situ) that would reduce transport of Ra downstream. With the use of $^{87}Sr/^{86}Sr$ and $\delta^{34}S_{SO4}$, it was noted that sulfate concentrations increase with distance from both evaporative effects and the oxidation of sulfide gas [17]. Elevated sulfate concentrations above 1,000 mg/L pose problems for dairy cows [22] while concentrations below 1,800 mg/L are recommended for Wyoming livestock to minimize the possibility of acute mortality [23].

Anoxic conditions are commonly found at depth in saturated, organic wetland sediments, where organic matter is a driving reductant. Reductive dissolution and subsequent release of sorbed or incorporated cations, such as Ra, would occur in the order hydrous Mn oxide (HMO) > hydrous Fe oxide (HFO) > sulfate minerals [24,25]. Additionally, bacterial enrichment cultures of Marcellus PW indicated the potential for halophilic anaerobic bacteria from the genus *Halanaerobium* to etch pits into barite minerals that increase the rate of its dissolution and subsequent release of any impurities back to the water column [26–29].

Issues related to the release of Ra from sorbed or incorporated mineral structures leads to the question whether wetlands or PWRPs may in fact provide a sustainable sequestration system for preventing mobility of Ra downstream. Inherent benefits to created or enhanced wetlands for wastewater treatment include achieving highly efficient contaminant removals through physical (increased retention time, settling, volatilization), chemical (oxidation, precipitation, adsorption, ion exchange) and biological (biodegradation, phytodegradation, evapotranspiration, plant uptake) means [30]. Reported radionuclide removals on created wetlands studied in Wyoming were only effectively achieving effluent goals 30% of the time, though removal mechanisms were not investigated in detail [31]. Wetlands also provide valuable wildlife habitat in semi-arid and arid regions where water is an otherwise scarce commodity [20]. Passive treatment by wetlands, namely free water surface designs, provides economically favorable returns compared to more elaborate treatment systems developed for PW such as advanced oxidation processes, electrocoagulation, membrane separation and distillation etc. [32–35]. The reduced costs associated with treatment wetlands, deduced from passive acid mine drainage (AMD) systems, stems from their reduced labor, reduced operational expertise, reduced chemical inputs, low maintenance necessary in remote regions, and lack of power requirements [36–40].

While the vegetation species present within a treatment wetland can introduce different reduction and oxidation (redox) conditions, it is apparently more important that a dense stand of vegetation is established [30]. Giant bulrush (*Schoenoplectus californicus*) are commonly used in treatment wetlands for maintaining negative sediment redox potentials as they produce minimal radial oxygen loss within the root zone [41–43]. These

anoxic conditions facilitate a habitat favorable for promoting dissimilatory sulfate reduction (-100 to -250 mV) which is conducive for the precipitation of recalcitrant sulfide minerals that can act as a sink for incorporation of metal impurities [44]. Conversely, cattails (*Typha*), notably the species *Typha angustifolia*, generate substantial radial oxygen loss within the rhizosphere which provides a conducive habitat for heterotrophic aerobic bacteria (HAB) (>100 mV) [42,45].

The objectives of this study were to 1) determine the efficacy of the PWRPs downstream of the NPDES discharges for removing Ra and other TDS components necessary for enhanced beneficial use, 2) gain a greater understanding of Ra sediment associations within PWRPs and with depth under anoxic conditions. The first two objectives are necessary to 3) identify PWRP functions that could be enhanced for optimal polishing of PW near the NPDES discharges to best protect human and ecosystem health downstream.

Materials and Methods

Site description

This study took place in remote O&G fields in Wyoming that are dominated by semi-arid sagebrush drainage regions that ultimately discharge to two larger perennial rivers fed by mountainous upstream regions. The study region receives an average of 230 mm of precipitation annually (www.climate.gov). The O&G fields are simultaneously

utilized for cattle rangelands and wildlife habitat. O&G extraction is regionally well-established with development of some of the major formations occurring in the 1950s. Due to increasing age of formation development and enhanced oil recovery processes flushing the formations, regional PW to O&G ratios (upwards of 116 from one permit) are much higher than the average US ratios of 7-10 barrels of PW per barrel of O&G [46]. In accordance with wildlife propagation as a beneficial use exemption under 40 CFR § 435 Subpart E, the U.S. Fish and Wildlife Service were involved in creating PWRPs for migratory birds within the Discharge C PW stream (Figure 1). The term wetland is used loosely within this study (both from a regulatory and ecological perspective) to describe the ponding and vegetated conditions within the PW discharge streams. O&G operators are not responsible for maintaining the wetlands once PW discharges and, thus, stream flows cease. Therefore, the wetlands are not legally defined as such under the Clean Water Act Section 404 and are instead referred to as PWRPs throughout.

Three O&G PW treatment facilities, referred to as Discharge A (DA-D), Discharge B (DB-D), and Discharge C (DC-D), and their naturally-dry ephemeral discharge receiving streams were sampled in November 2018 (Figure 1). A total of 19 GPS-located sites were sampled including 5 PWRP sites, 1 playa lake, and 1 control site wetland (CSW) not impacted by O&G produced water discharges. “D” denotes the discharge outfall, “W” denotes within the PWRP, and “US” and “DS” denote location upstream and downstream, respectively. DB-100m and DC-100m denote a sample that was taken 100 m downstream of the respective discharge (DB-D and DC-D). Site specificity is not disclosed in agreement with private landowner and O&G operator access. These study sites have been previously described in detail by McDevitt et al.

(2019, 2020b) in which, DA-D was referred to as DB-4.0, DB-D as DB-2.0, and DC-D as DC-1 (Table S1) [16,17]. A more detailed site description is included in the Supplemental Information.

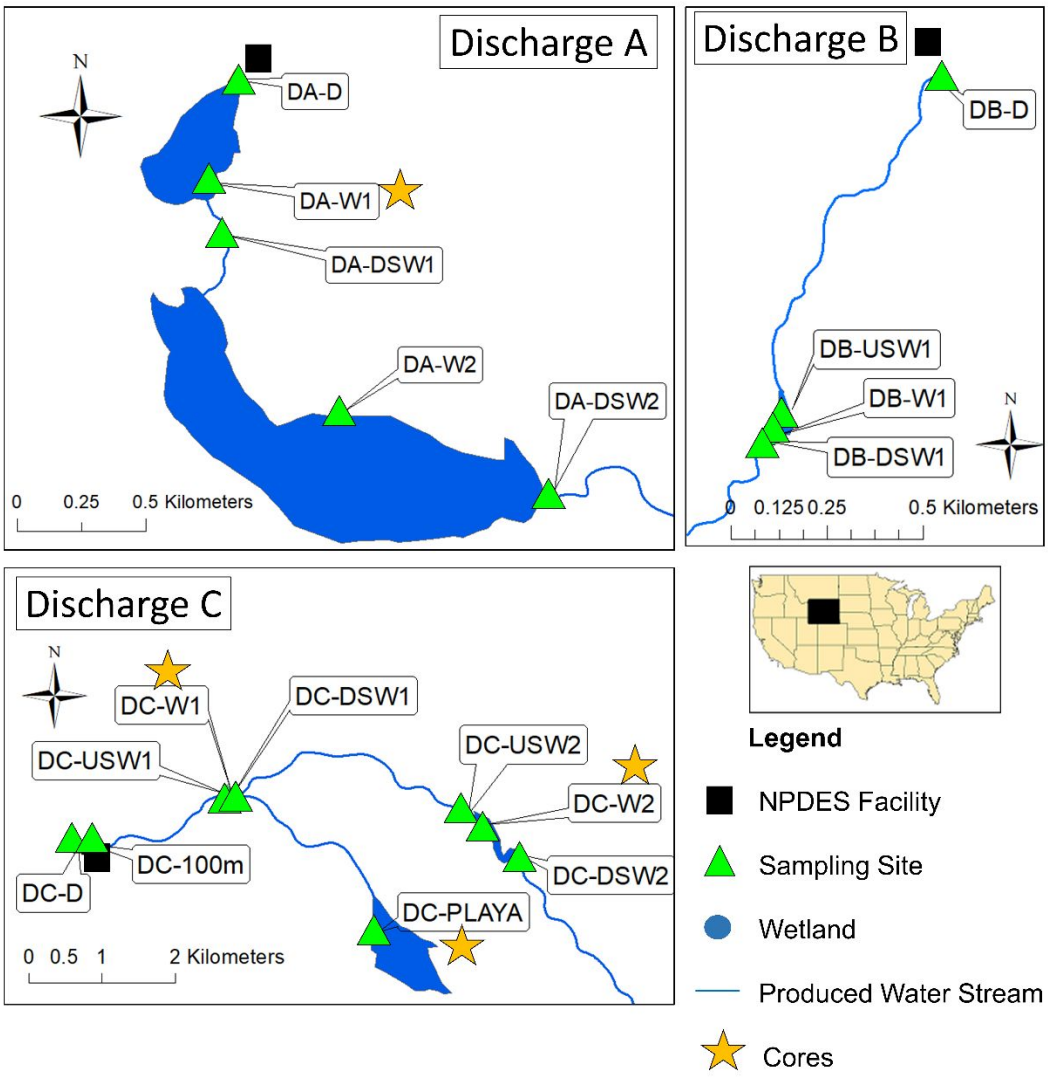

Figure 1. Map of the remote study region in Wyoming O&G fields. Three NPDES facilities (DA-D, DB-D, DC-D) and their PWRP complexes were studied. Water, sediment, and vegetation samples were collected in November 2018.

Treatment at all three facilities (DA-D, DB-D and DC-D) was similar. According to the NPDES permits, fluids from the wells flow into a three-phase separator (oil-gas-water) from which the PW flows through a series of settling/skim ponds for floating oil removal prior to NPDES discharge to surface water. Facility DA-D discharges an average 1.5 million L treated PW/day, DB-D discharges an average 310,000 L treated PW/day, and DC-D discharges an average 4.5 million L treated PW/day. Study site PW effluents are low TDS (~1,000 – 4,000 mg/L) compared to most U.S. produced waters. Discharge regulations are limited to specific conductance of 7,500 µS/cm, TDS of 5,000 mg/L, Cl of 2,000 mg/L, SO_4 of 2,500 mg/L, ^{226}Ra of 2.22 Bq/L (60 pCi/L), oil and grease of 10 mg/L, and a pH range of 6.5 to 9. While it was not quantified, sulfide in regional produced waters was an issue at all discharges sampled and required use of personal monitors in previous sampling campaigns. From permits, estimated annual sulfide (as H_2S) loads were 66,800 kg/year for DA-D, 6,900 kg/year for DB-D, and 133,000 kg/year for DC-D.

Field Sampling

Field sampling represents a snapshot in time of water and sediment chemistry and vegetative uptake since only one sampling event took place in November 2018, limiting seasonal or long-term interpretation of results. Hanna probe measurements (temperature, SC, DO and pH), water samples and grab sediment samples were collected at all 19-GPS located sites. Water samples were collected using 0.45-µm cellulose acetate membrane syringe filters and additionally preserved to a pH < 2 with trace-grade nitric acid for cation and trace metal analysis.

Four-inch diameter push-tube cores were collected (n=5) of varying depth adjacent to grab sediments (DA-W1, DC-W1, DC-W2, DC-PLAYA, CSW). Vegetation in the form of roots,

leaves and seeds, where possible, were collected in coordination with sediment cores (n=11). Cattail (*Typha*) vegetation was preferred for collection, but in areas where there were no cattails, existing vegetation in the form of grasses or bulrush sedges (*Cyperaceae*) was collected.

All samples were contained in coolers on ice until shipment to the laboratory where water samples and grab sediments were then refrigerated to 4°C and sediment cores and vegetation were kept frozen until analysis. Additional field sampling details are included in the Supplemental Information.

Laboratory analysis of samples

Filtered water samples were measured for major anions (Cl, SO_4, Br, NO_3, PO_4) by ion chromatography (IC) and filtered, acidified water samples were measured for major cations and trace metals by Inductively Coupled Plasma Optical Emission Spectrometry (ICP-OES). Check standards, USGS M-228 and T-235, standard reference samples for ICP-OES, and duplicate samples were measured every 10 samples and were within 2% RSD for each analyte measured.

Grab sediments were dried, crushed and measured by gamma spectrometry on a Canberra small anode germanium gamma ray spectrometer (SAGe). ^{226}Ra activity was measured as the average of the three daughter product activities: 295.22, 351.93 and 609.31 keV peaks, while ^{228}Ra was measured via the 911.20 keV ^{228}Ac peak. Grab sediments were also analyzed for total carbon (TC), total inorganic carbon (TIC), and by difference, total organic carbon (TOC), at Colorado State University and methodology details are included in the Supplemental Information.

Sediment cores were extracted from push tube cores while frozen and cut into 2 cm depth intervals. Immediately following, frozen sediment sections were transported into an anaerobic

chamber for further processing. Frozen sediments thawed within the anaerobic chamber and were then removed for centrifugation at 10,000 RPM for 20 minutes at 4°C. Back inside the anaerobic chamber, porewaters were extracted utilizing 0.45 μm cellulose acetate membrane syringe filters. Dissolved oxygen, temperature, pH, conductivity, and oxidation-reduction potential (ORP) were measured in the porewaters. Remaining wetsediments were frozen until dry by freeze drier. Dry sediments were then processed similarly to grab sediments and analyzed by gamma spectrometry. Porewaters were measured for major anions, cations and trace metals by IC and ICP-OES.

A select subset of sediment core samples (n=15, 3 depths/core) were subjected to an operationally defined 5-step leaching procedure modified from previous studies to understand Ra associations within PWRP sediments [16,47,48]. A solution to sediment ratio of 20:1 was employed to remain within detection limits for major cation analysis of leachates by ICP-OES. The leach steps were as follows:

1. Ultra-pure distilled water and shaking for 24 hours targeting soluble salts
2. 1 M ammonium acetate buffered to pH 8 by ammonium hydroxide and shaking for 12 hours targeting exchangeable cations
3. 0.1 M sodium pyrophosphate ($Na_4P_2O_7$) and shaking for 12 hours targeting organic matter-sorbed cations
4. 8% trace grade glacial acetic acid and shaking for 12 hours targeting carbonates by dissolution
5. 0.1 M trace grade hydrochloric acid and shaking for 12 hours targeting iron and manganese oxides and iron sulfide minerals by dissolution

The sediment residue remaining after the final leaching step is operationally assumed to maintain recalcitrant sulfate minerals such as barite that could coprecipitate Ra. After each step, samples were centrifuged, leachates filtered, and solid residues dried and measured for ^{226}Ra and ^{228}Ra by gamma spectrometry. A subset of these sediment samples (n=8) was analyzed by X-ray diffraction (XRD) for mineralogy. Additional details are included in the Supplemental Information.

Vegetation samples were thawed, cleaned using ultra-pure distilled water baths and Triton™ X-100 surfactant [49]. Vegetation was separated into roots, leaves/stems, and seeds, if present, freeze dried and measured by gamma spectrometry for ^{226}Ra and ^{228}Ra. Additional vegetation preparation details are included in the Supplemental Information.

Results & Discussion

Inorganic water chemistry

The PW effluent concentrations from three NPDES facilities were within regulatory limits for permitted discharges for all inorganic constituents measured (Table S2). McDevitt et al. (2020) presents a more comprehensive dataset of these discharges and their PW streams that included 10 sampling events from 2013-2016. From that data, and in agreement with data presented herein, the dominating compositions of these PW effluents are SO_4 and Na, followed by Ca. The high SO_4 compositions of these O&G effluents set them apart from brines of much higher TDS and Cl content as in the Appalachian Basin as well as other Western U.S. formations such as the Williston Basin in North Dakota [48,50,51]. Discharges A and B had much higher TDS concentrations compared to Discharge C. SO_4 concentrations were approximately 1,800 and

2,000 mg/L in both DA-D and DB-D, respectively, while DC-D SO_4 concentrations were much lower around 460 mg/L. CSW SO_4 and Cl concentrations were, as expected, lower with 318 mg/L and 6 mg/L, respectively. Cation composition at CSW was dominated by both Ca (44 mg/L) and Mg (41 mg/L). Notably, as previously reported, Ba and Sr concentrations are comparably low in these study site PW effluents compared to other O&G formations [16,17,52–54]; Ba concentrations remained near detection limits the entire sampling transect (<0.01 mg/L). Ba concentrations in DC-D effluents (0.14 mg/L) were approximately double those of DA-D (0.04 mg/L) and DB-D (0.05 mg/L). Sr concentrations at all sites ranged between 2 and 10 mg/L with all three discharge Sr concentrations around 5 mg/L. Because of high SO_4 concentrations, barite and celestite precipitation may occur prior to PW discharge leading to reduced dissolved Ba and Sr concentrations.

Major anions and cations (SO_4, Cl, and Na) in PW streams DA and DB increase with distance downstream (Figure 2). McDevitt et al. (2019) determined solute concentration factors for SO_4 upwards of 2.5 within 1 km of DC-D and DB-D. Similarly, SO_4 concentrations in this study more than doubled from DA-D to DA-DSW2 approximately 2 km downstream. It is important to note that assessing SO_4 concentrations alone, treated produced water from DA-D and DB-D is not suitable for use as a sole source of livestock drinking water which is recommended to have SO_4 concentrations less than 1,000 mg/L [22,23]. During sampling events, livestock were observed drinking water near DA-D and DC-D and a herd of pronghorn were observed drinking water near DA-D. It is not known if the wildlife and livestock use these PW discharges as a sole drinking water source year-round. Additionally, Cl concentrations from DA-D and DB-D, and along the entirety of the DB PW stream, are elevated above recommended livestock drinking water guidelines of < 250 mg/L. Sodium concentrations from DA-D and along

the entire DA PW stream are elevated above the livestock guideline of < 1,000 mg/L. Constant $^{87}Sr/^{86}Sr$ along the PW streams supported evaporation leading to concentrations, within regulatory limits at the outfall, that exceeded both drinking water standards and agricultural guidelines downstream [17]. Currently, regulations only apply to PW discharged at the NPDES outfall and do not apply to the PW post-discharge. Monitoring and reporting of NPDES effluents are conducted in accordance with individual permits that can vary by NPDES discharge. Surprisingly, on a finer DC PW stream distance scale (more sample points <15 km from DC-D), concentrations for major ions did not increase as appreciably as previously reported [16–18]. SO_4 concentrations increased approximately 135 mg/L from DC-D to DC-DSW2 (~6 km downstream). This could be due in part to the time of year (November) sampled. Although the DA PWRPs were covered in a sheet of ice during sampling, the DA PW stream increasing TDS concentrations indicate the most evidence for evaporation. Overall, major anion and cation data do not indicate abatement (via coprecipitation) of these PW effluent constituents with flow through the existing PWRPs.

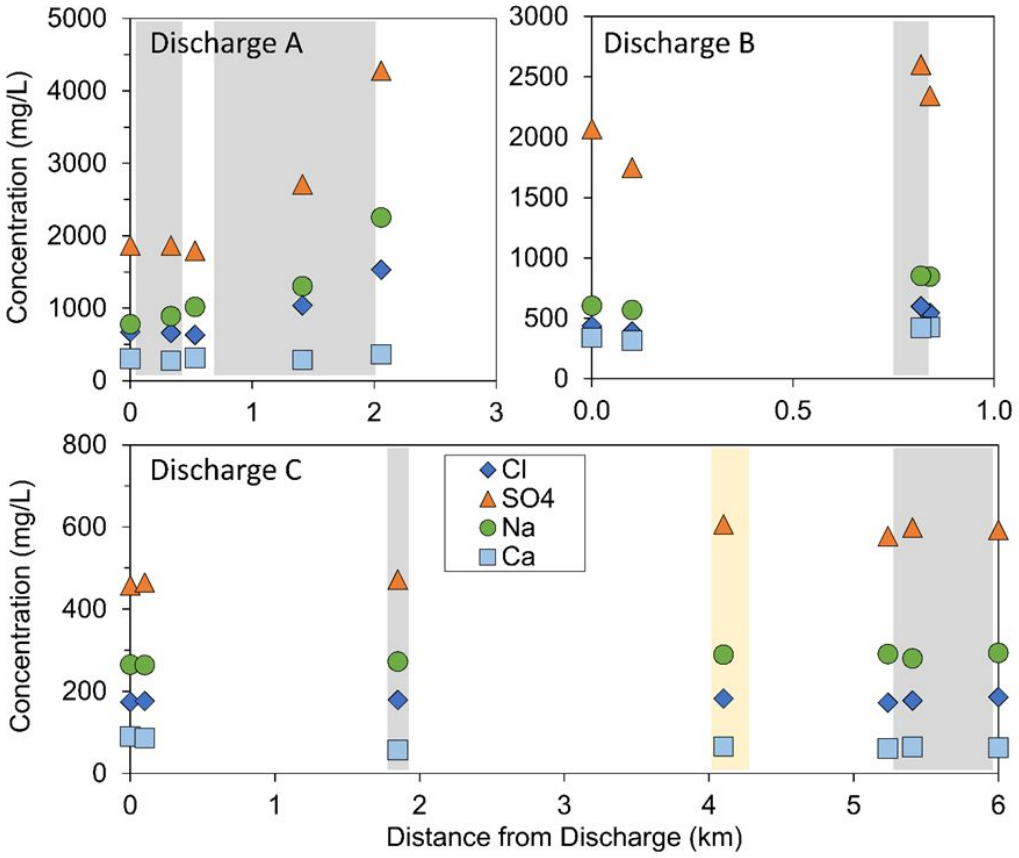

Figure **2:** Major ions (Cl, SO_4, Na and Ca) plotted versus distance from the respective NPDES discharge. Gray bars on the plots indicate the presence of a PWRP. The light-yellow bar indicates the presence of a playa lake (DC-PLAYA) created from a diversion of the DC PW stream.

Oxidation of hydrogen sulfide gas is likely occurring along the PW streams which was supported by decreasing $\delta^{34}S_{SO4}$ with increasing distance from the discharges [17]. Hydrogen sulfide is a regulated effluent parameter at DA-D and is known to be elevated at both DB-D and DC-D. A constructed wetland for PW treatment in the Pitchfork Field in Wyoming noted SO_4 concentrations increasing through the wetland as hydrogen sulfide concentrations decreased [31]. Oxidation of hydrogen sulfide gas to elemental sulfur occurs in the presence of oxygen, which increased with distance in the PW stream (Figure S1). Elemental sulfur (S) can then be

efficiently oxidized under aerobic conditions by chemolithotrophs to SO_4, which may play a role in increasing SO_4 concentrations with distance downstream. To round out the S cycle, SO_4 transported to anoxic conditions can then be reduced through dissimilatory SO_4 reduction by sulfate-reducing microorganisms where SO_4 acts as the terminal electron acceptor and yields sulfide. Sulfide can precipitate key recalcitrant minerals known to sorb metals in wetland or anaerobic systems [31,42,55]. Under anoxic conditions, up to approximately 35% SO_4 reduction, calcium carbonate minerals can be undersaturated and unstable due to the oxidation of organic matter which releases CO_2, causing a decrease in pH [56]. Sulfate reduction can account for upwards of 50% carbonate mineral dissolution[57]. Sulfide (which can accumulate in sediments with low Fe concentrations) oxidation releases protons also contributing to a decrease in pH, potentially causing further carbonate mineral dissolution.

Most interesting is a finding from Caswell et al. (1992) where the oxidation of sulfide to sulfate under aerobic conditions by oxygenic/anoxygenic photosynthetic cyanobacteria removes CO_2 from the water, increasing the pH and adding dissolved oxygen. This in turn increases the carbonate mineral saturation index and can lead to the common formation of carbonate terraces that we most noted at sites DA-D and DB-D and comprised the majority of sediments collected near NPDES discharges in McDevitt et al. (2019). The most common microorganisms responsible for this phenomenon are from the genus *Chloroflexus* and *Oscillatoria*. From a companion study, microbial abundance data derived from 16S rRNA gene sequencing indicated Chloroflexia was the most dominant taxa present at DC-D (19%) and DC-100m (35%) (Figure S2) [58]. Smaller abundance of this taxa was observed at sites DA-W1, DA-W2 and DB-D. DA-D could have relatively high abundance of Chloroflexia too, but amplification issues with samples from that site limits any conclusions. On the other hand, Deltaproteobacteria were also present in

high relative abundance at most PW stream sites, though this abundance increased with distance along the DC PW stream [58]. Deltaproteobacteria species (beyond the scope of this study and companion study) *Desulfovibrio cuneatus* and *Desulfovibrio desulfuricans*, have previously been documented to reduce barite minerals containing ^{226}Ra, releasing a small fraction (<0.1%) of the Ba and similarly trending ^{226}Ra to the water column [28].

Grab sediment Ra activities and attenuation downstream

McDevitt et al. (2019) reported low average dissolved total Ra (^{226}Ra+^{228}Ra) from 2013-2016 in NPDES effluents from DA-D as 0.29 Bq/L, DB-D as 2.12 Bq/L, and DC-D as 0.43 Bq/L which led to elevated radium activities in near-outfall sediments compared to downstream and background sites[16]. In this study, radium activities in grab sediments at all NPDES discharges were elevated above background sediments collected at CSW (44 ± 0.59 Bq/kg ^{226}Ra, 90 ± 4.18 Bq/kg Total Ra) (Figure 3, Table S2). Additionally, all NPDES discharge sediments, and many PW stream sediments, were elevated compared to the EPA Action Level (40 CFR 192) threshold for the upper 15 cm of sediments where ^{226}Ra sediment activities cannot exceed 185 Bq/kg above background activities (~74 Bq/kg). This Action Level is thus approximately set at 259 Bq/kg. The highest measured Total Ra sediment activity was sampled from DB-100m upwards of 4289 ± 68 Bq/kg, higher than what was previously observed by McDevitt et al. (2019) around 3500 Bq/kg. DC-D sediments had significantly less Ra activity than DA-D and DB-D, reflecting activities (648 ± 33 Bq/kg Total Ra) similar to what was previously reported for this site sampled in 2016 [16]. The lower DC-D sediment Ra activity may relate to reaching the sediment capacity to incorporate or sorb more Ra since a previous Ra mass balance estimated that 95% of the annual Ra load was transported beyond 100 m from the discharge [16].

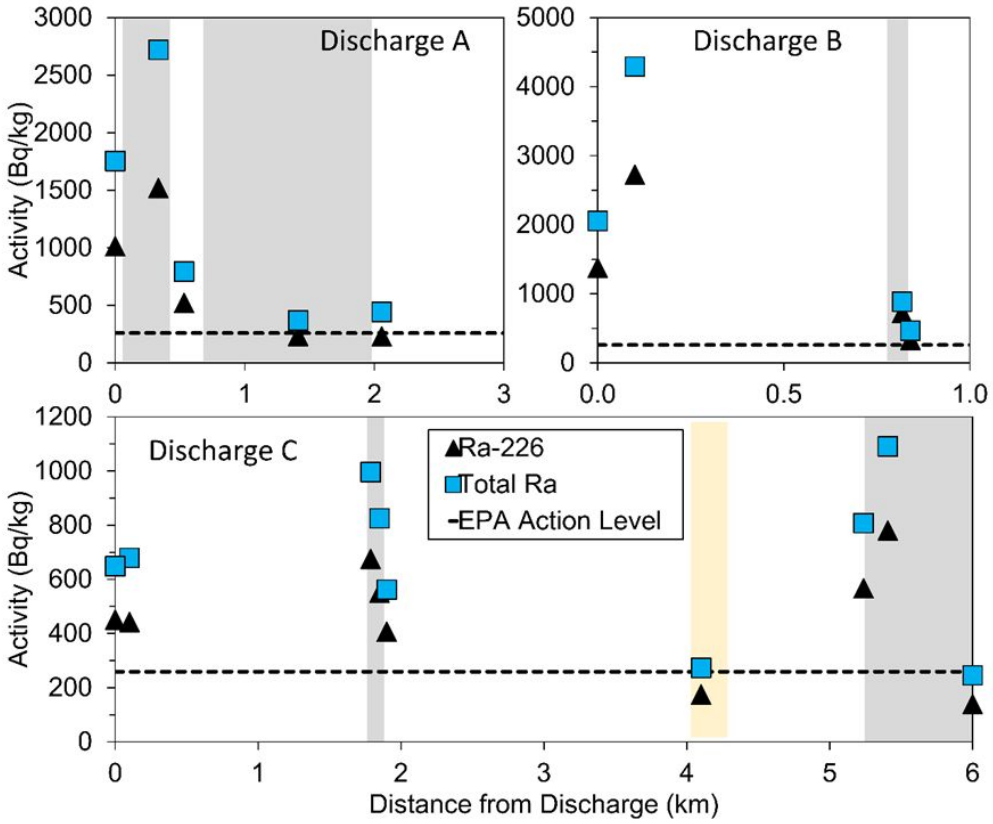

Figure **3:** ^{226}Ra and total Ra (^{226}Ra+^{228}Ra) activities plotted versus distance from the respective NPDES discharge. The EPA Action Level indicated by the horizontal dashed line is set at 259 Bq/kg (185 Bq/kg above background sediment activities (~74 Bq/kg)). Gray bars indicate a PWRP and the light-yellow bar indicates the playa lake (DC-PLAYA) diversion on the DC PW stream.

With increasing distance downstream of the discharges, Ra attenuation profiles at the higher sampling resolution in this study do not appear similar to those in McDevitt et al. (2019). Previously, Ra attenuation profiles along the PW stream transect reflected a trend reminiscent of sorption behavior as a removal mechanism. On this finer distance scale, Ra activities are elevated within every PWRP sampled apart from DC-W1 and DA-W2, which was largely unvegetated and more akin to a large pond. Likely, the PWRPs that exhibit relatively elevated Ra activities are trapping fine Ra-associated particles that settle and accumulate to activities higher than both

sediments collected upstream and downstream. Upon accumulation, the fine particles may then be buried, chemically or biologically transformed, and sorbed/incorporated species potentially made available for plant root uptake. While total suspended solids (TSS) data was not collected, anecdotally, water samples were much easier to filter at the outfall of the PWRPs than water samples collected upstream or within.

The bioavailability of the Ra in the sediments is a function of the Ra phase – whether sorbed, co-precipitated, aqueous, and ultimately to what it may be sorbed or incorporated (i.e. clays, organic matter, HMO, HFO, SO_4 or CO_3 minerals) [59]. From McDevitt et al. (2019), Ra was significantly associated with calcium carbonate sediment compositions. As grab sediment TC, TIC, and TOC data would suggest (Table S3), Ra sediment activity profiles with distance trend in accordance with the TC-dominating TIC compositions [58]. The only location where the trend does not hold is DC-USW2, DC-W2 and DC-DSW2 where Ra sediment activities follow that of TOC concentrations (as % dry weight) which dominate the TC compositions (upwards of only ~4%). PWRP (DA-W2, DB-W1, DC-W1 and DC-W2) sediment TOC compositions were higher compared to respective upstream and downstream sediments. Organic matter sorption of Ra is less studied than other sorption or coprecipitation Ra attenuation mechanisms. However, studies have shown that Ra was enriched in soil organic matter and that organic matter was able to sorb 10 times more Ra than clay minerals [59–61].

Ra associations in PWRP sediments with depth

Understanding Ra associations within O&G PWRP sediments, and any changes in those associations with depth and distance downstream, is valuable information for regulators and

operators seeking better system designs for Ra treatment. Regionally, Ra associations will differ based upon varying PW chemistry, varying equilibrium conditions and varying nutrient cycling behavior. In the study site region, high PW SO_4/H_2S discharges lead to the dominating importance of the S cycle for discussing Ra associations.SO_4 concentration profiles vary with sediment core depth in PWRPs DC-W1, DC-W2, and DC-PLAYA (Figure 4, Figure 5, Table S4). DC-PLAYA SO_4 concentrations increase with depth, DC-W1 SO_4 concentrations remain elevated at depth, and DC-W2 SO_4 concentrations decrease approximately two magnitudes from the upper to lower sediment sections (1,100 to 9 mg/L, respectively). The difference in the profile trends with depth between DC-W1 and DC-W2 may be evidenced in microbial community differences as indicators of redox conditions. Chloroflexia had a higher abundance in more upstream DC PW stream grab sediments, where sulfide concentrations were higher and dissolved oxygen concentrations were lower compared to downstream water samples (Figure S2). With increasing distance downstream of DC-D, SO_4 and DO concentrations increase (Table S4)while Deltaproteobacteria abundance in surface sediments increased. The depletion of SO_4 concentrations in the DC-W2 sediment core agree with this microbial community respiration, assuming the surface sediment microbial community remains similar at some depth in the sediment profile. The DC-W2 core porewater Fe and SO_4 concentrations follow opposite trends at what appears may be the O_2/H_2S interface from redox data (Figure 4, Table S4). This trend may indicate that as SO_4 is reduced under anoxic conditions, iron oxide minerals are also reduced, releasing Fe as a dissolved species. While the Fe core profile is irregular, the highest Fe porewater concentrations correlate with the lowest porewater ORP measurements. The subsequent dissolved Fe concentration decrease with depth potentially indicates formation of iron sulfide minerals. Dissolved Mn porewater concentrations (Figure S3, Table S4) follow a

relatively similar trend to dissolved Fe both with notable concentration increases at 4 cm and 10 cm depths where corresponding ORP measurements indicate reducing conditions. In that case, Ra may be released from small amounts of sulfate minerals and sorbed by organic matter or iron sulfide mineral surfaces as demonstrated in previous studies [62].

CSW sediments near the core surface represent anoxic conditions (<0 mV) (Figure 6, Table S4) and ORP gradually increases with depth. CSW SO_4 concentrations increase with the corresponding ORP increases to concentrations that are a magnitude larger than all other core porewater SO_4 concentrations. CSW Na-SO_4 type porewaters reached conductivities upwards of 20 mS/cm at 25 cm depth. This finding was surprising due to the low conductivity of the CSW surface water sample (0.90 mS/cm, 81 mg/L Na, and 318 mg/L SO_4).

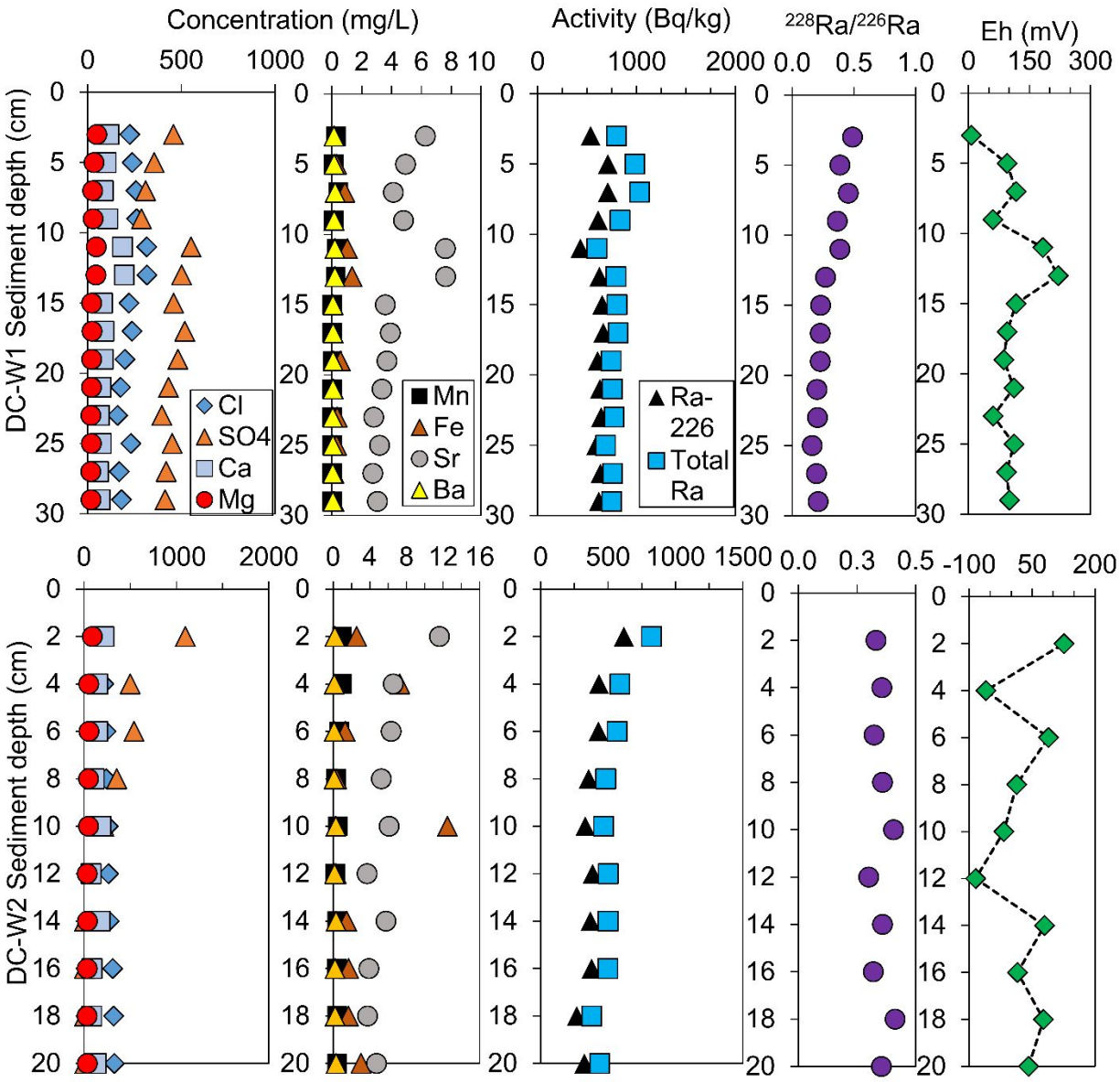

Figure **4:** DC-W1 and DC-W2 sediment core porewater major ion concentrations, sediment Ra activities (^{226}Ra and Total Ra), and ^{228}Ra/^{226}Ra activity profiles with depth. See Figure S3 for scaled Ca, Mg, Ba and Mn profiles.

455

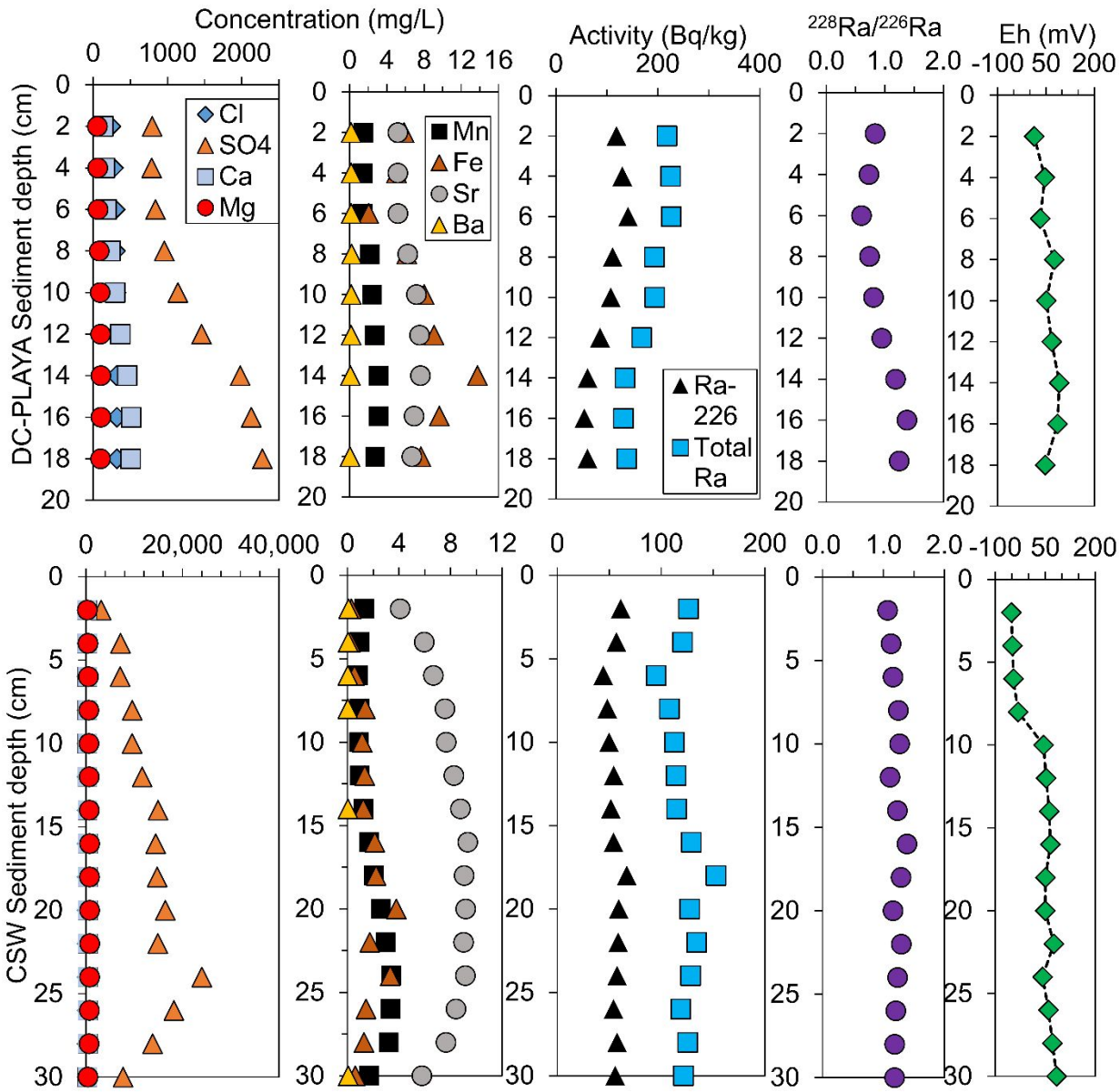

Figure **5:** DC-PLAYA and CSW sediment core porewater major ion concentrations, sediment Ra activities (^{226}Ra and Total Ra), and ^{228}Ra/^{226}Ra activity profiles with depth. See Figure S3 for scaled Ca, Mg, Ba, and Mn profiles.

456

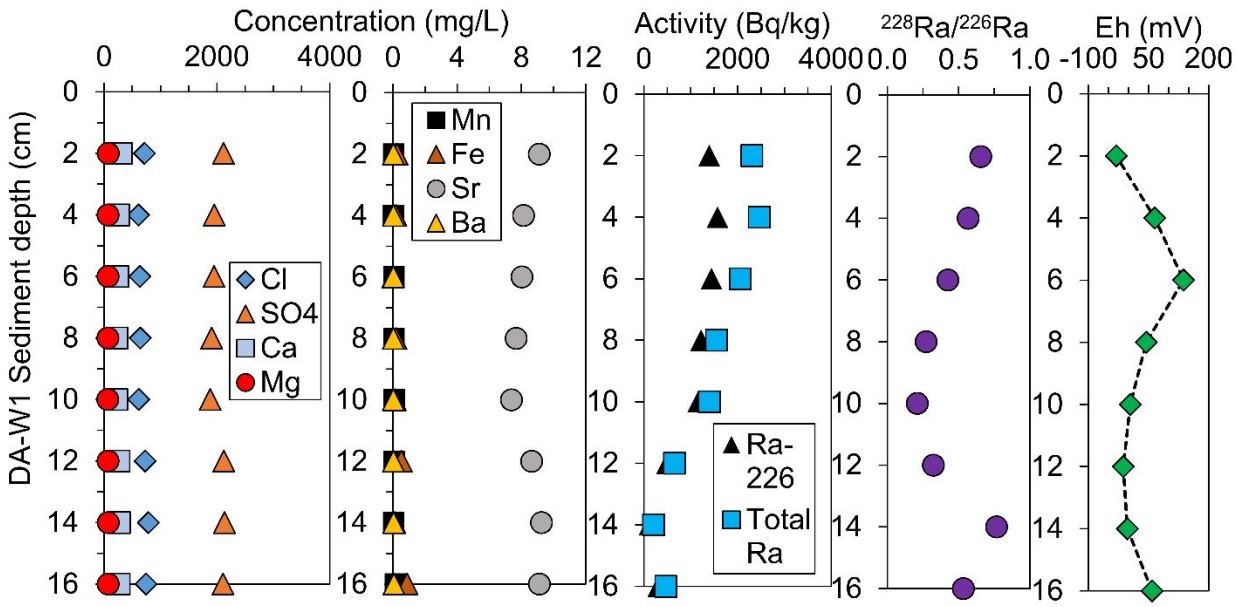

Figure **6:** DA-W1 sediment core porewater major ion concentrations, sediment Ra activities (^{226}Ra and Total Ra), and ^{228}Ra/^{226}Ra activity profiles with depth. See Figure S3 for scaled Ca, Mg, Ba and Mn profiles.

It is not easily discernible from porewater concentrations and Ra sediment activity trends if there are significant correlations for Ra sequestration (Table S4). DC-W1 Ra profiles remain fairly consistent with depth except for a small decrease at ~10 cm associated with an increase in many of the ions thought to be correlated to Ra attenuation by sorption or coprecipitation: Fe, Sr, Ca, and SO_4 [16,62–65]. DC-W2 Ra profiles decreased only slightly with depth. Notably, sediment Ra activities with depth in DC-W1 and DC-W2 sediments are nearly as elevated (~1000 Bq/kg Total Ra) as the DC-D discharge core collected in October 2016, despite being located almost 2 km and 5 km downstream, respectively [16]. All PW stream cores, DA-W1, DC-W1, and DC-W2 have Ra sediment activities at depth that exceed those measured in the CSW background core (highest Total Ra measured 153 Bq/kg at 16-18 cm depth). DC-PLAYA sediment Ra activities are only slightly elevated above those of the CSW core (highest Total Ra measured 226 Bq/kg at DC-PLAYA 4-6 cm depth). DA-W1 total Ra activities, however, were twice as elevated as those

of DC-W1 and DC-W2 near the surface (upwards of 2,460 Bq/kg) and decreased to approximately 200 Bq/kg, within a shallow depth of 14 cm, to less than the EPA Action level threshold (Figure 6). This decrease could be associated with plant root uptake at a depth of approximately 15 cm as there were dense stands of cattails present at site DA-W1 [66]. Ca porewater concentrations in DC-W1 are about half those of the 2016 DC-D core. Sequential leaching in McDevitt et al. (2019) confirmed calcium carbonate compositions of sediments decreased significantly with increasing distance downstream. The $^{228}Ra/^{226}Ra$ ratio profiles in both the CSW and much of the DC-PLAYA cores indicate a ratio (~1) indicative of background sediments not impacted by disposal of O&G PW [67–70]. Reference site grab sediment samples from McDevitt et al. (2019) $^{228}Ra/^{226}Ra$ ratios ranged from 1.3-1.7. All other cores represented ratios <1 and potentially indicate contribution of O&G PW ^{226}Ra.

Ra association and characterization through operationally-defined sequential leaching

An operationally-defined sequential leaching procedure was completed to more quantifiably identify Ra sequestration mechanisms (Figure 7). DA-W1 represents the closest sampling site to the DA-D outfall. As hypothesized based on findings from McDevitt et al. (2019), the upper-most leached core sediments (DA-W1 2-4 cm) lost the most Ca and Ra during the carbonate-targeted leaching step of all sediments sequentially leached (39% Ra loss) (Table S5). This result was expected due to the vast carbonate terraces present at this site and the ~50% sediment mass dissolved during this step. With increasing depth in the DA-W1 core profile, Ra association with the exchangeable fraction of clays and organic matter increased. This trend was correlated with loss of the most sediment Sr and Ba in the deepest core section during the exchangeable ion-targeted leach step. In contrast to the more oxic upper two sediment sections,

anoxic DA-W1 12-14 cm lost the majority of sediment Fe in the oxide/sulfide-targeted leaching step and the majority of its S in the soluble salts-targeted step. Redox potential differences within the same sediment core offer insights that anoxic conditions may cause more recalcitrant minerals (SO_4>CO_3) formed under oxic conditions to become unstable[56], re-solubilizing sorbed or incorporated Ra.

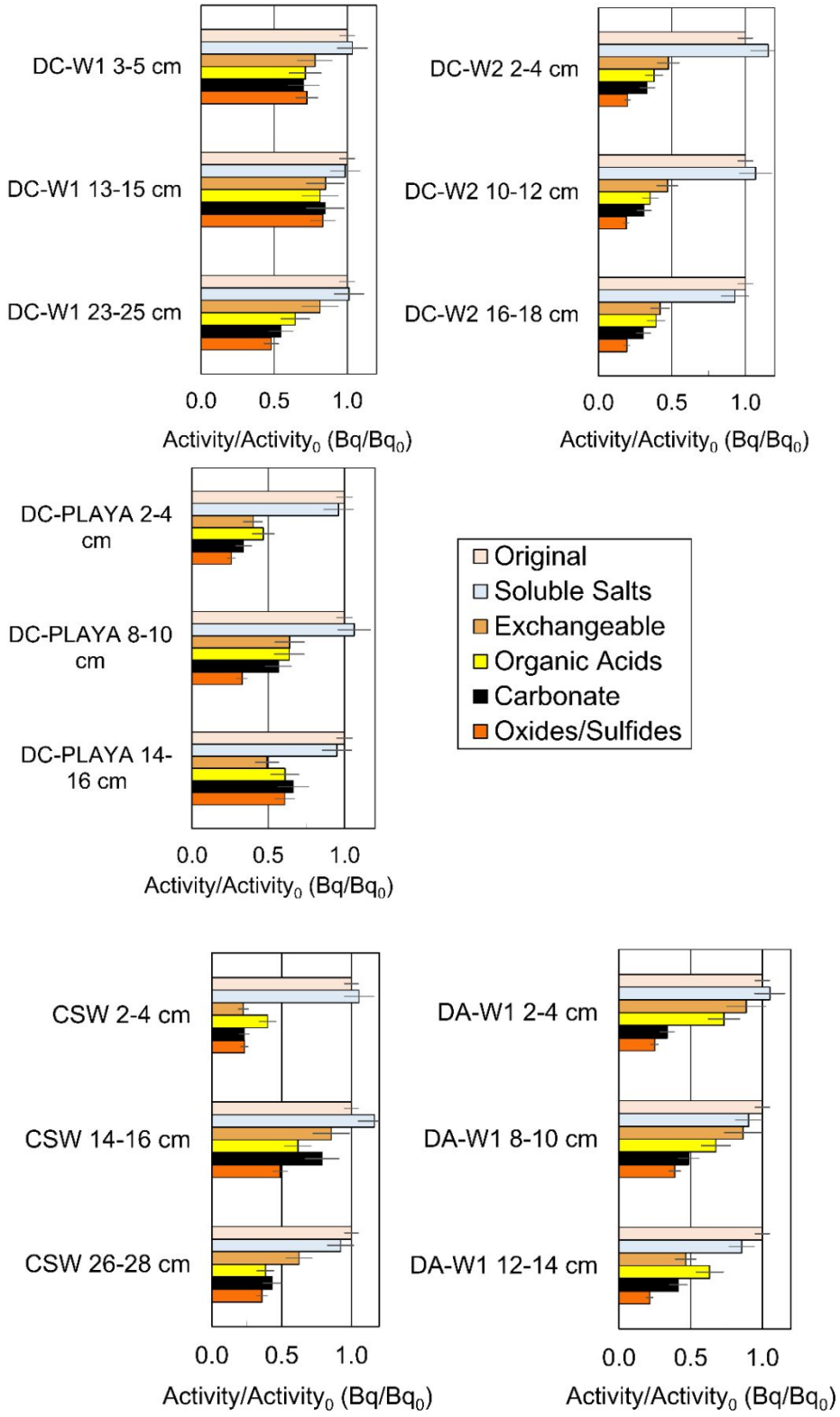

Figure **7:** Leaching data for select sediment core depth. Ra was analyzed post-leach step on solid sample residues. Data is presented as residue activity (Bq) normalized to the initial

activity and is also presented in Table S5.

DC-D grab sediment leach data presented in McDevitt et al. (2019) indicated that 75% of the sediment Ra was associated with carbonate minerals which constituted >97% of the sample mass. In that study, sediment Ra along the 30 km transect could be adequately modeled assuming all Ra was incorporated or sorbed onto calcium carbonate solid solutions. This was due to the precipitation of approximately 3 orders of magnitude more calcium carbonate mass than sulfate solid solutions. DC-W1 and DC-W2 PWRP cores lost little Ra within the carbonate-targeted leaching step, even from surface sediments, though calcite and dolomite PHREEQC-calculated[16] saturation indices generally indicated supersaturation throughout both cores (Figure S4). For the PHREEQC calculations, bicarbonate concentrations were estimated from the porewater charge balance differences. From XRD analysis, DC-W1 core sediments, notably those at the sediment surface, indicated dominance of calcium carbonate minerals comprising upwards of 75% (Table S6). Oxic DC-W1 core sediments still maintained >50% of the sediment Ra after steps 1-5, with one section (DC-W1 13-15 cm) still maintaining ~85% of the sediment Ra after all 5 steps (the greatest percentage of Ra maintained of all sediment sections analyzed). Any remaining Ra after all leach steps is operationally assumed to indicate the sequestration of Ra in relatively recalcitrant minerals such as barite (SO4>CO3). XRD of the DC-W1 13-15 cm leach residue supported the presence of remnant calcium carbonate minerals but did not detect sulfate minerals, though amorphous sulfate mineral compounds would not have been detected by XRD. From PHREEQC saturation indices, DC-W1 porewaters indicated supersaturation of barite throughout the sediment core (celestite was undersaturated), whereas DC-W2 porewaters indicated undersaturation of barite from 16-20 cm in depth. XRD indicated trace amounts of barite or celestite in both cores at some depths but less than 1% composition in quantified

analyses (Table S6). Anoxic DC-W2 PWRP conditions indicate Ra associations within the more labile exchangeable ion fraction of sediments (>50%), in coordination with large mass losses of Ca (much less than in DC-W1 core sediments), Ba, and Sr during the second leaching step. XRD analysis indicated DC-W2 sediments comprised larger amounts of clay minerals such as montmorillonite and illite, known to sorb large amounts of Ra. Sorption of Ra by clay minerals is enhancedwhen large amounts of quartz and other silicates are present, also supported by XRD analysis (Table S6) [59,71,72]. This may also be partly due to the more reducing conditions that cause the release of Ra from small amounts of more unstable calcium carbonate or sulfate minerals (the majority of sediment S lost during leaching occurred in step one targeting soluble salts). The more oxidizing conditions in DC-W1 indicate Ra may still be incorporated in a sulfate/carbonate mineral (majority of sediment S lost during leaching occurred in step four targeting carbonate minerals). Sulfide minerals were not detected at quantifiable levels by XRD in any samples and could not be modeled with PHREEQC due to a lack of sulfide porewater concentration. However, the inconsistency in $Fe(OH)_3$ saturation within the DC-W2 core (Figure S4) paired with labile, water-soluble S and anoxic conditions, potentially demonstrate that sulfate reduction is causing sulfide accumulation in the low Fe sediments without the formation of sulfide minerals[57]. DC-PLAYA surface sediments behaved more similarly to DC-W2. However, one depth section (DC-PLAYA 14-16 cm), corresponding with a spike in Fe porewater concentration and an increasing SO_4 concentration, maintains 61% of the sediment associated Ra after all leach steps 1-5.

CSW sediments with depth maintained a maximum of 36% of the sediment Ra although conditions were increasingly oxidizing with depth beyond 8 cm and SO_4 concentrations in porewaters were high (upwards of 24,000 mg/L at a depth of 24 cm). CSW sediment porewater

concentrations, however, demonstrate Ba concentrations below detection, limiting thermodynamic favorability of barite coprecipitation of Ra. Anoxic sediment core sample CSW 2-4 cm relatively lost the most Ra of all samples after leaching step two targeting the exchangeable fraction of the sediment. However, the original ^{226}Ra activity was only 57 Bq/kg and represents an original activity over a magnitude less than some of the PWRP core sediments. All three sediment core depth CSW leachates indicate S sediment concentrations were easily leachable and between 77% and 88% S mass loss occurred during the application of ultra-pure distilled water, while Ba, Sr, and Ca were mostly leached as exchangeable ions. Sequentially leached CSW sediments indicated large counting errors associated with Ra gamma measurement due to low original sediment activities and the small mass of sample.

Overall, sequential leaching data indicates that organic matter sorption of Ra may not be as significant in attenuating downstream sediment Ra activities as originally hypothesized. While some of the organic matter-sorbed Ra could have been lost during the second leaching step targeting exchangeable ions, the lack of a clear association between Ra and organic matter may be due in part to the overall low TOC sediment compositions (measured in grab sediments) even within PWRPs (Table S3). The highest TOC composition was only approximately 4% in DC-W2 grab sediment, compared to other reported PWRP sediment ranges (14-50% organic matter [73]) that significantly sorbed ^{228}Ra (upwards of 30%) and smaller amounts of ^{226}Ra (upwards of 3%). From Dowdall and O'Dea (2002), there was no significant difference between ^{226}Ra activities within the easily oxidizable organic matter fraction or the iron oxide fraction of the soils. Additionally, carbonate minerals at the sediment surface and near discharges represent a major sink for Ra [16,74–77]. However, with increasing sediment depth, and with increasing distance from the discharge, carbonate minerals decrease in Ra sequestration importance, as was also deduced

with increasing distance from NPDES discharges by McDevitt et al. (2019). Ultimately, for ecological and human health, it would be ideal if Ra was mostly associated with sulfide minerals (determined with relatively how much Ra is lost during leach step 5), or even more recalcitrant, sulfate solid solutions such as $(Ba,Ra)SO_4$ or $(Ba,Sr,Ra)SO_4$ (determined with relatively how much Ra remains after step 5) [78–80]. These solid solutions represent a Ra sink that is more difficult to dissolve under rapidly changing equilibrium conditions, and thus prevents Ra mobility and bioavailability within the PW streams.

Vegetative uptake of Ra from produced water for beneficial use

From vegetation samples analyzed for Ra accumulation, background wetland (CSW) cattail roots accumulated much less ^{226}Ra (7 Bq/kg dry weight) compared to vegetation collected from areas impacted by PW discharges (upwards of 880 Bq/kg dry weight) (Table S7). The slope of the linear correlation of ^{226}Ra in the plant material to ^{226}Ra in the substrate represents the concentration ratio (C_r), defined as the Ra activity in Bq/kg dry weight in the plant material to Ra activity in Bq/kg dry weight of the sediment. Ra activity in the sediment section at 5-cm depth was utilized in the calculation as previous studies indicate all roots are within 0-20 cm depth for *Typha* species that have deeper root systems than grasses with highest rooting density at depths 0-2.5 cm [81–83]. It is important to note that it has been shown that plants accumulate Ra more in roots>stems>shoots>leaves as can be evidenced at most study sites with the exception of DA-W1, DB-100m,DB-W1 where leaves>roots

It has been debated whether Ra in the plant increases linearly with Ra in the substrate, as a constant concentration ratio would assume, or whether it plateaus at some maximum [66,84,85]. Our data indicate that in general, Ra in the plant increases with Ra in the substrate and a plateau

in root samples may be reached (Figure 8A). The assumption of linearity in soil to plant transfer factors was previously supported when contaminant (U, Th, ^{226}Ra) activities utilized in the regression were wide ranging (~ 2 magnitudes) [86]. Previous studies theorized that C_r decreases as a function of substrate concentration due to saturation phenomenon by Ca and other exchangeable alkaline earth metals at plant roots limiting Ra adsorption and its biological uptake rate [84,87] . Additionally, the strong negative correlation between the partitioning coefficient (K_d) and C_r for contaminants (Cs, Se, I, Pb and U) indicated the importance for considering the ions available in soluble form, not total soil concentration [85]. Madruga et al. (2001) demonstrated the need to consider the exchangeable ion fraction of the total soil concentration that is bioavailable to plants and that C_r values calculated based on the exchangeable ^{226}Ra were an order of magnitude higher than those based on total soil ^{226}Ra activities [88]. From our leaching data step two, utilizing 1 M ammonium acetate to flush exchangeable Ra, $C_{r\text{-exchangeable}}$ values for the plant material were calculated and range from 1.3 to 11 times larger than the respective total sediment ^{226}Ra C_r. $C_{r\text{-exchangeable}}$ values decrease with increasing percentage of exchangeable ^{226}Ra (Figure 8B), similar to findings by Simon and Ibrahim (1990) and Williams (1982). While the exchangeable ion fraction is an important consideration for bioaccumulation, no significant effect of soil type was observed on the Ra C_r [66]. Decreasing Ra $C_{r\text{-exchangeable}}$ as a function of increasing exchangeable sediment Ra, indicates that the more bioavailable the Ra in the sediment, the less the plants are acting as a Ra sink, which may have implications for increased Ra transport.

The ERICA Assessment Tool[89] was utilized to estimate radiation dosing to vascular plants and other aquatic life based on default C_r values (Bq/kg fresh weight/ Bq/L) and K_d value (L/kg). At all sites, including background CSW, insect larvae, mollusks and zooplankton

exceeded the recommended conservative weight absorbed dose (10 μGy/h), amphibians and birds exceeded the recommended dose at all PWRP sites, and mammals did not exceed the 10 μGy/h at any study sites. It is important to note that study site K_d values (~420 L/kg) determined from discharge permit aqueous Ra activities and measured sediment activities were approximately 34 times smaller than the default ERICA K_d value of 14,000 L/kg. The K_d and C_r values are highly dependent on water chemistry, soil composition (clays, Ra-incorporating minerals, Ra-sorbing minerals), and redox parameters which affect the bioavailability of Ra. Despite adjusting the K_d value to calculated values, predicted vascular plant Ra accumulation at DC-D (~570 Bq/kg dry weight) greatly exceeded measured plant Ra accumulation (~76 Bq/kg dry weight), and thus overestimated vascular plant dosage. As a big-picture, consolidated, adjustable tool ERICA can provide a rapid assessment of potential negative consequences to aquatic life but results should be confirmed by training the tool with measured values prior to potential decision-making.

Cattails provide a main food source and nesting habitat for muskrats (*Ondatra zibethicus*). A previous study reported significant ^{226}Ra accumulation in cattail vegetation downstream of uranium tailing drainage and local muskrat bones (mean of 344.9 Bq/kg, n=36) compared to two control sites (mean of 80.3 Bq/kg, n=9) [90]. Muskrats are currently experiencing widespread population declines in North America [91]. Assuming the average mass of a muskrat is 1.14 kg [92], a muskrat consumes approximately one-third of its body weight in cattail vegetation daily, and the highest total Ra measured in cattail vegetation was 150 Bq/kg, we estimate a maximum daily muskrat Ra activity intake of 57 Bq/day. Compared to the cattail vegetation reported at background site CSW of 7 Bg/kg, a muskrat could be estimated to consume 2.7 Bq/day, approximately 20 times less than the highest PWRP site. Estimated mean $C_{r\text{-}wo/soil}$ (Ra in

whole organism (Bq/kg fresh weight)/Ra in soil (Bq/kg dry weight)) for Ra in herbivorous mammals is 6.1E-3 [93]. Utilizing the highest soil total Ra activity in this study of 4,289 Bq/kg we conservatively estimate whole organism muskrat Ra activity as 26 Bq/kg. Further, by multiplying whole organism Ra activity by a factor of 38 [93] we can estimate Ra activity in the muskrat tissue as 994 Bq/kg. From ERICA, 994 Bq/kg fresh weight would lead to an estimated weight absorbed dose of 142 μGy/h, a range in which mice populations reportedly experienced decreased fecundity and decreased early survival rates and male pig fertility significantly decreased. Ra incorporated into animal tissues can pose severe health issues due to radioactive decay linked to lung and bone cancers [94]. In terms of Ra sequestration, substantial uptake of Ra in cattails and other plants does not represent an ideal treatment mechanism if plants are allowed to be consumed by wildlife..

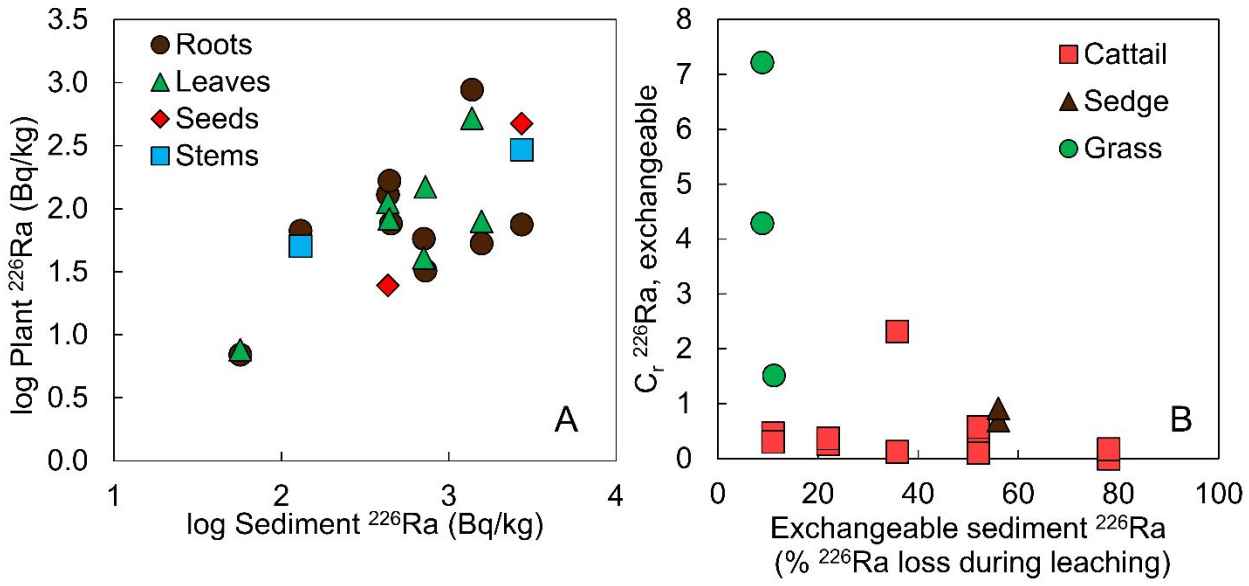

Figure **8: A)** Log of the ^{226}Ra activity in plant anatomy versus log sediment ^{226}Ra activity from the 5-cm section of the respective sediment sample and **B)** Exchangeable-normalized C_r for ^{226}Ra versus percentage exchangeable sediment ^{226}Ra measured during leaching step two in the 5-cm corresponding core section or as reported in McDevitt et al. (2019). Data is also presented in Table S7.

Conclusions

In this remote region of Wyoming, annually, billions of Bq of radium activity are permitted for release to ephemeral draws that represent consistent sources of low-level Ra contamination to sediments. PWRPs downstream provide a successful treatment for the oxidation of PW organic contaminants which were observed to degrade with distance downstream in a companion study [58]. However, inorganic PW concentrations, namely Na, Cl, and SO_4 were not reduced throughout the PWRP series downstream of NPDES discharge outfalls; instead, SO_4 concentrations increased substantially downstream of Discharge A. Ra, specifically, was observed to accumulate more within PWRP sediments compared to sediments collected at the respective PWRP outfall, indicating PWRPs may provide a sink for capturing fine particle-associated Ra. Unlike previous findings of Ra associated with grab sediment

carbonate minerals near NPDES discharges, Ra was less associated with carbonate minerals both with depth and with increasing distance downstream of discharges. The decreasing association of Ra with carbonate minerals could offer a preferred, long-term, Ra sequestration mechanism if incorporated into sulfate minerals (best) or recalcitrant iron sulfide minerals (redox-controlled). Samples that were leached and retained the most Ra after leaching steps 1-5 (i.e. DC-W1) also corresponded with samples that had the most oxic porewater measurements. Anoxic PWRP conditions likely induce instability in both sulfate and carbonate minerals as could be seen in the bulk loss of Ra, Ba, Sr, and Ca in the exchangeable ion-targeted leach step and the loss of S in the water-soluble ion-targeted step. Microbial community and vegetation community changes may induce some of the varying redox conditions both with depth and distance downstream. The correlation between Ra recalcitrance and oxic conditions supports the treatment need for PWRPs to remain oxygenated for best Ra capture and bioavailability prevention.

Moving forward, treatment optimization can likely occur by maintaining one aerobic polishing PWRP near the NPDES discharge outfall, which already contain a series of settling tanks or ponds prior to discharge of net alkaline PW [40]. Ideally, this wetland would allow for volatilization of remaining hydrogen sulfide gas post-treatment, increase in DO, and ample retention time for Ra-associated particle settling. A small baffle could be installed to allow aeration through a waterfall and a dense stand of cattail vegetation could be transplanted to aid in maintaining oxic redox conditions. Cattail vegetation in this location would require a physical barrier to prevent wildlife consumption and habitat use. Upkeep on this aerobic PWRP could include ORP readings in real-time by low maintenance, solar-powered sensors in sediments within the PWRP to ensure oxidizing conditions and grab sediment sample collection from the PWRP outfall to ensure low Ra activities and minimal mobilization. Should redox conditions

change from oxic to anoxic, and Ra activities downstream of the PWRP increase, sediments within the PWRP may need additional oxygenation. Passive Ra treatment by oxic wetlands can provide a relatively cheap addition to minimal PW treatment intended for beneficial use occurring in remote regions of Wyoming; however, it is imperative that conditions remain oxic for Ra sequestration that best protects downstream human and ecological health.

Acknowledgements

The authors would like to acknowledge O&G collaborators and landowners without whom sampling could not have taken place. The authors would also thank Malichai Jones and Gregory Laporte from The Pennsylvania State University for aid in laboratory sample preparation. Student support was funded by NSF:AIR 1640634, NSF:AIR-REU Supplement, and NSF Wastewater Sediment grant 1703412. Funding was also provided by the Environmental Defense Fund and Colorado State University Water Center.

Conflict of Interest

The authors have no conflicts of interest to declare.

References

1 C. Clark and J. Veil, U.S. Produced water volumes and management practices, *Groundw. Prot. Counc.*, 2015, 119.

2 A. J. Kondash, N. E. Lauer and A. Vengosh, The intensification of the water footprint of hydraulic fracturing, *Sci. Adv.*, , DOI:10.1126/sciadv.aar5982.

3 C. L. Coonrod, Y. B. Yin, T. Hanna, A. Atkinson, P. J. J. Alvarez, T. N. Tekavec, M. A. Reynolds and M. S. Wong, Fit-for-purpose treatment goals for produced waters in shale

oil and gas fields, *Water Res.*, 2020, **173**, 115467.

4 D. Elsworth, C. J. Spiers and A. R. Niemeijer, Understanding induced seismicity, *Science (80-.).*, 2016, **354**, 1380–1381.

5 F. C. Dolan, T. Y. Cath and T. S. Hogue, Assessing the feasibility of using produced water for irrigation in Colorado, *Sci. Total Environ.*, 2018, **640**–**641**, 619–628.

6 EPA, Study of Oil and Fas Extraction Wastewater Management, https://www.epa.gov/eg/study-oil-and-gas-extraction-wastewater-management.

7 USGS, Mendenhall Research Fellowship Program 18-26. Reuse and treatment of high-salinity waters produced from hydrocarbon wells, https://www.usgs.gov/centers/mendenhall/18-26-reuse-and-treatment-high-salinity-waters-produced-hydrocarbon-wells.

8 U.S. Department of Energy, Department of Energy Invests $4.6M in Produced Water Treatment, https://www.energy.gov/fe/articles/department-energy-invests-46m-produced-water-treatment.

9 EPA, Water Reuse Action Plan, https://www.epa.gov/waterreuse/water-reuse-action-plan.

10 A. J. Kondash, J. Hoponick, E. Lambertini, L. Feinstein, E. Weinthal, L. Cabrales and A. Vengosh, Science of the Total Environment The impact of using low-saline oil fi eld produced water for irrigation on water and soil quality in California.

11 H. Miller, K. Dias, H. Hare, M. A. Borton, J. Blotevogel, C. Danforth, K. C. Wrighton, J. A. Ippolito and T. Borch, Reusing oil and gas produced water for agricultural irrigation: Effects on soil health and the soil microbiome, *Sci. Total Environ.*, , DOI:10.1016/j.scitotenv.2020.137888.

12 K. A. Patnode, E. Hittle, R. M. Anderson, L. Zimmerman and J. W. Fulton, Effects of

high salinity wastewater discharges on unionid mussels in the allegheny river, Pennsylvania, *J. Fish Wildl. Manag.*, 2015, **6**, 55–70.

13 N. Wang, J. L. Kunz, D. Cleveland, J. A. Steevens and I. M. Cozzarelli, Biological Effects of Elevated Major Ions in Surface Water Contaminated by a Produced Water from Oil Production, *Arch. Environ. Contam. Toxicol.*, 2019, **76**, 670–677.

14 T. A. Blewett, P. L. M. Delompré, C. N. Glover and G. G. Goss, Physical immobility as a sensitive indicator of hydraulic fracturing fluid toxicity towards Daphnia magna, *Sci. Total Environ.*, 2018, **635**, 639–643.

15 T. A. Blewett, A. M. Weinrauch, P. L. M. Delompré and G. G. Goss, The effect of hydraulic flowback and produced water on gill morphology, oxidative stress and antioxidant response in rainbow trout (Oncorhynchus mykiss), *Sci. Rep.*, 2017, **7**, 46582.

16 B. McDevitt, M. McLaughlin, C. A. Cravotta, M. A. Ajemigbitse, K. J. Van Sice, J. Blotevogel, T. Borch and N. R. Warner, Emerging investigator series: radium accumulation in carbonate river sediments at oil and gas produced water discharges: implications for beneficial use as disposal management, *Environ. Sci. Process. Impacts*, 2019, **21**, 324–338.

17 B. McDevitt, M. C. McLaughlin, D. S. Vinson, T. J. Geeza, J. Blotevogel, T. Borch and N. R. Warner, Isotopic and element ratios fingerprint salinization impact from beneficial use of oil and gas produced water in the Western U.S., *Sci. Total Environ.*, , DOI:10.1016/j.scitotenv.2020.137006.

18 M. McLaughlin, T. Borch, B. McDevitt, N. R. Warner and J. Blotevogel, Water Quality Assessment Downstream of Oil and Gas Produced Water Discharges Intended for Beneficial Reuse in Arid Regions, *Sci. Total Environ.*, 2020, **713**, 136607.

19 M. C. McLaughlin, J. Blotevogel, R. A. Watson, B. Schell, T. A. Blewett, E. J. Folkerts, G. G. Goss, L. Truong, R. L. Tanguay, J. Lucas and T. Borch, Mutagenicity assessment downstream of oil and gas produced water discharges intended for agricultural beneficial reuse, *Sci. Total Environ.*, 2020, **715**, 136944.

20 P. Ramirez, Oil field-produced water discharges into wetlands: Benefits and risks to wildlife, *Environ. Geosci.*, 2005, **12**, 65–72.

21 P. J. Ramirez, *Contaminants in Oil Field Produced Waters Discharged into the Loch Katrine Wetland Complex , Park County , Wyoming and Their Bioconcentration in the Aquatic Bird Food Chain*, Cheyenne, 1993.

22 B. Swistock, Interpreting Drinking Water Tests for Dairy Cows, https://extension.psu.edu/interpreting-drinking-water-tests-for-dairy-cows.

23 M. Raisbeck, S. Riker, C. Tate, R. Jackson, M. Smith, K. Reddy and J. Zygmunt, *Water Quality for Wyoming Livestock & Wildlife*, 2008.

24 C. A. J. Appelo and D. Postma, *Geochemistry, Groundwater and Pollution*, A.A. Balkema Publishers, Amsterdam, 2nd edn., 2005.

25 K. Van Sice, C. A. Cravotta, B. McDevitt, T. L. Tasker, J. D. Landis, J. Puhr and N. R. Warner, Radium attenuation and mobilization in stream sediments following oil and gas wastewater disposal in western Pennsylvania, *Appl. Geochemistry*, 2018, **98**, 393–403.

26 B. Ouyang, D. M. Akob, D. Dunlap and D. Renock, Microbially mediated barite dissolution in anoxic brines, *Appl. Geochemistry*, 2017, **76**, 51–59.

27 K. K. Falkner, G. P. klinkhammer, T. S. Bowers, J. F. Todd, B. L. Lewis, W. M. Landing and J. M. Edmond, The behavior of barium in anoxic marine waters, *Geochim. Cosmochim. Acta*, , DOI:10.1016/0016-7037(93)90366-5.

28 E. R. Elizabeth J. P. Phillips, Sulfate-Reducing Bacteria Release Barium and Radium from Naturally Occurring Radioactive Material in Oil-Field Barite, *Geomicrobiol. J.*, 2001, **18**, 167–182.

29 D. Renock, J. D. Landis and M. Sharma, Reductive weathering of black shale and release of barium during hydraulic fracturing, *Appl. Geochemistry*, 2016, **65**, 73–86.

30 N. Nijhawan and J. E. Myers, Constructed treatment wetlands for the treatment and reuse of produced water in dry climates, *8th SPE Int. Conf. Heal. Saf. Environ. Oil Gas Explor. Prod. 2006*, 2006, **2**, 553–560.

31 P. C. Caswell, D. Gelb, S. A. Marinello, J. C. Emerick and R. R. Cohen, Component performance evaluation of constructed surface flow and wetlands cells for produced water treatment in the pitchfork field, Wyoming, *Proc. - SPE Annu. Tech. Conf. Exhib.*, 1992, **Pi**, 435–444.

32 Y. Sun, D. Wang, D. C. W. Tsang, L. Wang, Y. S. Ok and Y. Feng, A critical review of risks, characteristics, and treatment strategies for potentially toxic elements in wastewater from shale gas extraction, *Environ. Int.*, 2019, **125**, 452–469.

33 B. Akyon, M. McLaughlin, F. Hernández, J. Blotevogel and K. Bibby, Characterization and biological removal of organic compounds from hydraulic fracturing produced water, *Environ. Sci. Process. Impacts*, 2019, **21**, 279–290.

34 D. E. Freedman, S. M. Riley, Z. L. Jones, J. S. Rosenblum, J. O. Sharp, J. R. Spear and T. Y. Cath, Biologically active filtration for fracturing flowback and produced water treatment, *J. Water Process Eng.*, 2017, **18**, 29–40.

35 H. Chang, T. Li, B. Liu, R. D. Vidic, M. Elimelech and J. C. Crittenden, Potential and implemented membrane-based technologies for the treatment and reuse of flowback and

produced water from shale gas and oil plays: A review, *Desalination*, 2019, **455**, 34–57.

36 P. F. Ziemkiewicz, J. G. Skousen and J. Simmons, Long-term Performance of Passive Acid Mine Drainage Treatment Systems, *Mine Water Environ.*, 2003, **22**, 118–129.

37 P. F. Ziemkiewicz, J. G. Skousen, D. L. Brant, P. L. Sterner and R. J. Lovett, Acid Mine Drainage Treatment with Armored Limestone in Open Limestone Channels, *J. Environ. Qual.*, 1997, **26**, 1017.

38 P. Ziemkiewicz, J. Skousen and J. Simmons, Cost benefit analysis of passive treatment systems, *Proceedings, 22nd West Virginia Surf. Mine Drain. Task Force Symp.*

39 C. A. Cravotta and M. K. Trahan, Limestone drains to increase pH and remove dissolved metals from acidic mine drainage, *Appl. Geochemistry*, , DOI:10.1016/S0883-2927(98)00066-3.

40 R. S. Hedin, R. W. Nairn and R. L. P. Kleinmann, Passive treatment of coal mine drainage, *Inf. Circ. 9389*, 1994, 1–44.

41 C. L. Murray-Gulde, G. M. Huddleston, K. V. Garber and J. H. Rodgers, Contributions of Schoenoplectus californicus in a constructed wetland system receiving copper contaminated wastewater, *Water. Air. Soil Pollut.*, 2005, **163**, 355–378.

42 B. L. Alley, B. Willis, J. Rodgers and J. W. Castle, Seasonal performance of a hybrid pilot-scale constructed wetland treatment system for simulated fresh oil field-produced water, *Water. Air. Soil Pollut.*, , DOI:10.1007/s11270-013-1639-5.

43 M. N. Josselyn, S. P. Faulkner and W. H. Patrick, Relationships between seasonally wet soils and occurrence of wetland plants in California, *Wetlands*, 1990, **10**, 7–26.

44 D. B. Kosolapov, P. Kuschk, M. B. Vainshtein, A. V. Vatsourina, A. Wießner, M. Kästner and R. A. Müller, Microbial processes of heavy metal removal from carbon-deficient

effluents in constructed wetlands, *Eng. Life Sci.*, 2004, **4**, 403–411.

45 T. Matsui Inoue and T. Tsuchiya, Interspecific differences in radial oxygen loss from the roots of three Typha species, *Limnology*, 2008, **9**, 207–211.

46 K. Guerra, K. Dahm and S. Dundorf, *Oil and gas produced water management and beneficial use in the Western United States*, Denver, 2011.

47 T. T. Phan, R. C. Capo, B. W. Stewart, J. R. Graney, J. D. Johnson, S. Sharma and J. Toro, Trace metal distribution and mobility in drill cuttings and produced waters from Marcellus Shale gas extraction: Uranium, arsenic, barium, *Appl. Geochemistry*, 2015, **60**, 89–103.

48 B. W. Stewart, E. C. Chapman, R. C. Capo, J. D. Johnson, J. R. Graney, C. S. Kirby and K. T. Schroeder, Origin of brines, salts and carbonate from shales of the Marcellus Formation: Evidence from geochemical and Sr isotope study of sequentially extracted fluids, *Appl. Geochemistry*, 2015, **60**, 78–88.

49 W. R. Edwards and K. E. Smith, Exploratory Experiments on the Stability of Mineral Profiles of Feathers, *J. Wildl. Manage.*, 1984, **48**, 853–866.

50 N. R. Warner, C. A. Christie, R. B. Jackson and A. Vengosh, Impacts of shale gas wastewater disposal on water quality in Western Pennsylvania, *Environ. Sci. Technol.*, 2013, **47**, 11849–11857.

51 M. S. Blondes, K. D. Gans, M. A. Engle, Y. K. Kharaka, M. E. Reidy, V. Saraswathula, J. J. Thordsen, E. L. Rowan and E. A. Morrissey, U.S. Geological Survey National Produced Waters Geochemical Database (ver. 2.3, January 2018).

52 E. C. Chapman, R. C. Capo, B. W. Stewart, C. S. Kirby, R. W. Hammack, K. T. Schroeder and H. M. Edenborn, Geochemical and strontium isotope characterization of

produced waters from marcellus shale natural gas extraction, *Environ. Sci. Technol.*, 2012, **46**, 3545–3553.

53 N. Abualfaraj, P. L. Gurian and M. S. Olson, Characterization of marcellus shale flowback water, *Environ. Eng. Sci.*, 2014, **31**, 514–524.

54 B. McDevitt, M. Cavazza, R. Beam, E. Cavazza, W. D. Burgos, L. Li and N. R. Warner, Maximum Removal Efficiency of Barium, Strontium, Radium, and Sulfate with Optimum AMD-Marcellus Flowback Mixing Ratios for Beneficial Use in the Northern Appalachian Basin, *Environ. Sci. & Technol.*, , DOI:10.1021/acs.est.9b07072.

55 Y. S. Han, T. J. Gallegos, A. H. Demond and K. F. Hayes, FeS-coated sand for removal of arsenic(III) under anaerobic conditions in permeable reactive barriers, *Water Res.*, 2011, **45**, 593–604.

56 J. W. Morse, Formation and Diagenesis of Carbonate Sediments, *Treatise on Geochemistry*, 2003, **7**, 67–85.

57 L. M. Walter, S. A. Bischof, W. P. Patterson and T. W. Lyons, Dissolution and recrystallization in modern shelf carbonates: evidence from pore water and solid phase chemistry, *Philos. Trans. - R. Soc. London, A*, 1993, **344**, 27–36.

58 M. C. McLaughlin, Colorado State University, 2019.

59 International Atomic Energy Agency, *The Environmental Behaviour of Radium : Revised Edition*, Vienna, 2014.

60 D. J. Greeman, A. W. Rose, J. W. Washington, R. R. Dobos and E. J. Ciolkosz, Geochemistry of radium in soils of the Eastern United States, *Appl. Geochemistry*, 1999, **14**, 365–385.

61 J. S. Nathwani and C. R. Phillips, Adsorption of Ra-226 by soils (I), *Chemosphere*, 1979,

5, 285–291.

62 M. A. Chen and B. D. Kocar, Radium Sorption to Iron (Hydr)oxides, Pyrite, and Montmorillonite: Implications for Mobility, *Environ. Sci. Technol.*, 2018, **52**, 4023–4030.

63 K. Van Sice, C. A. Cravotta, B. McDevitt, T. L. Tasker, J. D. Landis, J. Puhr and N. R. Warner, Radium attenuation and mobilization in stream sediments following oil and gas wastewater disposal in western Pennsylvania, *Appl. Geochemistry*, 2018, **98**, 393–403.

64 T. Zhang, R. W. Hammack and R. D. Vidic, Fate of Radium in Marcellus Shale Flowback Water Impoundments and Assessment of Associated Health Risks, *Environ. Sci. Technol.*, 2015, **49**, 9347–9354.

65 T. Zhang, K. Gregory, R. W. Hammack and R. D. Vidic, Co-precipitation of radium with barium and strontium sulfate and its impact on the fate of radium during treatment of produced water from unconventional gas extraction, *Environ. Sci. Technol.*, 2014, **48**, 4596–4603.

66 F. Carvalho, D. Chambers, S. Fesenko, W. S. Moore, D. Porcelli, H. Vandenhoven and T. Yankovich, *Environmental Pathways and Corresponding Models*, Vienna, 2014.

67 N. E. Lauer, N. R. Warner and A. Vengosh, Sources of Radium Accumulation in Stream Sediments near Disposal Sites in Pennsylvania: Implications for Disposal of Conventional Oil and Gas Wastewater, *Environ. Sci. Technol.*, 2018, **52**, 955–962.

68 P. Dresel and A. Rose, Chemistry and origin of oil and gas well brines in western Pennsylvania, *Pennsylvania Geol. Surv., 4th Ser. Open …*, 2010, 48.

69 E. L. Rowan, M. a. Engle, C. S. Kirby and T. F. Kraemer, Radium Content of Oil- and Gas-Field Produced Waters in the Northern Appalachian Basin (USA): Summary and Discussion of Data, *USGS Sci. Investig. Rep.*, 2011, 38 pp.

70 M. Asikainen, Radium content and the 226Ra228Ra activity ratio in groundwater from bedrock, *Geochim. Cosmochim. Acta*, 1981, **45**, 1375–1381.

71 P. Benes, P. Strejc and Z. Lukavec, Interaction of Radium with Freshwater Sediments and their Mineral Components. I.Ferrix hydroxide and quartz., *J. Radioanal. Nucl. Chem.*, 1984, **82**, 275–285.

72 P. Benes, B. Z. and P. Strejc, Interaction of Radium With Freshwater Sediments and their Mineral Components: III. Muscovite and Feldspar., *J. Radioanal. Nucelear Chem.*, 1986, **98**, 91–103.

73 M. Dowdall and J. O'Dea, 226Ra/238U disequilibrium in an upland organic soil exhibiting elevated natural radioactivity, *J. Environ. Radioact.*, 2002, **59**, 91–104.

74 M. J. Jones, L. J. Butchins, J. M. Charnock, R. A. D. Pattrick, J. S. Small, D. J. Vaughan, P. L. Wincott and F. R. Livens, Reactions of radium and barium with the surfaces of carbonate minerals, *Appl. Geochemistry*, 2011, **26**, 1231–1238.

75 D. S. Vinson, J. R. Lundy, G. S. Dwyer and A. Vengosh, Implications of carbonate-like geochemical signatures in a sandstone aquifer: Radium and strontium isotopes in the Cambrian Jordan aquifer (Minnesota, USA), *Chem. Geol.*, 2012, **334**, 280–294.

76 E. Curti, Coprecipitation of radionuclides with calcite: Estimation of partition coefficients based on a review of laboratory investigations and geochemical data, *Appl. Geochemistry*, 1999, **14**, 433–445.

77 D. Langmuir and A. C. Riese, The Thermodynamic Properties of Radium, *Geochim. Cosmochim. Acta*, 1985, **49**, 1593–1601.

78 P. Risthaus, D. Bosbach, U. Becker and A. Putnis, Barite scale formation and dissolution at high ionic strength studied with atomic force microscopy, *Colloids Surfaces A*

Physicochem. Eng. Asp., 2001, **191**, 201–214.

79 W. Shi, A. T. Kan, C. Fan and M. B. Tomson, Solubility of Barite up to 250 °C and 1500 bar in up to 6 m NaCl Solution, , DOI:10.1021/ie2020558.

80 C. W. Blount, Barite solubilities and thermodynamic quantities up to 300'C and 1400 bars, *Am. Mineral.*, 1977, **62**, 942–957.

81 S. L. Miao and F. H. Sklar, Biomass and nutrient allocation of sawgrass and cattail along a nutrient gradient in the Florida Everglades, *Wetl. Ecol. Manag.*, 1997, **5**, 245–264.

82 Y. M. Chun and Y. D. Choi, Expansion of Phragmites australis (Cav.) Trin. ex Steud. (common reed) into Typha spp. (cattail) wetlands in northwestern Indiana, USA, *J. Plant Biol.*, 2009, **52**, 220–228.

83 K. Sung, C. L. Munster, R. Rhykerd, M. C. Drew and M. Y. Corapcioglu, The use of vegetation to remediate soil freshly contaminated by recalcitrant contaminants, *Water Res.*, 2003, **37**, 2408–2418.

84 S. L. Simon and S. . Ibrahim, in *The Environmental Behaviour of Radium*, International Atomic Energy Agency, Vienna, 1990, pp. 545–599.

85 S. C. Sheppard and W. G. Evenden, The assumption of linearity in soil and plant concentration ratios: An experimental evaluation, *J. Environ. Radioact.*, 1988, **7**, 221–247.

86 P. Blanco Rodríguez, F. Vera Tomé and J. C. Lozano, About the assumption of linearity in soil-to-plant transfer factors for uranium and thorium isotopes and 226Ra, *Sci. Total Environ.*, 2002, **284**, 167–175.

87 A. R. Williams, *Biological uptake and transfer of radium-226: a review*, IAEA, International Atomic Energy Agency (IAEA), 1982.

88 M. J. Madruga, A. Brogueira, G. Alberto and F. Cardoso, 226Ra bioavailability to plants

at the Urgeirica uranium mill tailings site, *J. Environ. Radioact.*, 2001, **54**, 175–188.

89 N. Beresford, Norwegian Radiation Protection Agency, Environment Agency, Centre for Ecology and Hydrology, IRSN, Swedish Radiation Safety Authority and CIEMAT, ERICA 1.3.1.51, http://erica-tool.com/erica/erica-partners/.

90 M. A. Mirka, F. V. Clulow, N. K. Dave and T. P. Lim, Radium-226 in cattails, Typha latifolia, and bone of muskrat, Ondatra zibethica (L.), from a watershed with uranium tailings near the city of Elliot Lake, Canada, *Environ. Pollut.*, 1995, **91**, 41–51.

91 L. S. Ganoe, J. D. Brown, M. J. Yabsley, M. J. Lovallo and W. D. Walter, *Front. Vet. Sci.*, 2020, 7, 233.

92 T. L. Newell, Ondatra zibethicus, https://animaldiversity.org/accounts/Ondatra_zibethicus/, (accessed 9 January 2020).

93 IAEA, *Handbook of Parameter Values for the Prediction of Radionuclide transfer to wildlife*, Vienna, 2014.

94 Agency for Toxic Substances and Disease Registry, *Toxicological Profile for Radium*, Atlanta, 1990.